

Thermal performance analysis of thermoelectric radiant panel system for indoor space heating

Gaurav Mishra*, Satyendra Prajapati, Jyotirmay Mathur, Aneesh Prabhakar

Centre for Energy and Environment, Malaviya National Institute of Technology Jaipur, Jaipur, India
2021ren9565@mnit.ac.in

Abstract

The study is focused on the thermal performance analysis of a thermoelectric radiant heating panel (TERHP) system in a test chamber for cold climatic conditions. Three radiant panels with eight thermoelectric modules (TEM) each are installed on the three different walls of the study chamber to evaluate the performance of the panels to achieve the thermal comfort temperature inside the chamber of $1.2 \times 1.2 \times 2$ m. All TEMs in a single TE panel of size 0.75×0.50 m are attached in a triangular arrangement to obtain a uniform temperature. The water block is used as a heat sink to maintain the temperature difference between the cold and hot sides of TEMs. The water circulation circuit with the "I" configuration has been used. Hot water at a constant temperature is supplied to the water block, and cold water obtained at the outlet is collected and circulated back after thermoregulation in a closed loop. The experiment is conducted by supplying inlet water at 18°C and applying operating voltages to the TERHP system of 12 V, 16 V, and 20 V. The surface temperature of panels, mean radiant temperature, operative temperature, air temperature, heating capacity, and coefficient of performance are measured on these inputs.

Keywords - Thermoelectric module, Thermal performance, Radiant heating, Heating capacity, Low energy heating.

1. Introduction

A commitment to cut hydrofluorocarbon (HFC) consumption by 80% by 2047 was made when representatives from over 150 nations signed the Kigali Amendment in 2016. This would be a significant step in our attempts to lessen the effects of climate change since, if successful, it would prevent more than 0.4°C of global warming by the end of the century [1]. According to the IEA's 2019 report, India's energy demand for air conditioning is anticipated to triple by 2050. This points out the requirement for energy-efficient and sustainable air conditioning solutions [2]. Buildings account for a sizable portion of global energy consumption and carbon dioxide emissions. Hence, a new viable solution is required to tackle the above mentioned issues. Thermoelectric radiant cooling or heating systems for buildings can be a beneficial option due to its compact size, less maintenance, no use of refrigerant and long operating life.

A thermoelectric module (TEM) working on the Peltier effect has a thermoelectric element that is powered by direct current (DC). Depending on the direction of the current flow, TEM can transfer heat one way or another. The possible application options of this technology are the integration of thermoelectric (TE) radiant panels on the ceiling and walls of a building. Numerous studies have been carried out to assess and optimize the performance of thermoelectric systems.

The experiments performed by Cosnier et al. [3] confirmed the feasibility of heating air using thermoelectric modules in the system. The investigation shows that coefficient of performance (COP) of 2 can be easily reached by applying a current of 4-5 A while keeping the hot and cold side temperature difference of $5-10^\circ\text{C}$. Shen et al. [4] have developed a mathematical model to optimize the TE radiant panel design for better cooling and heating performance. Results show that for better performance of the radiant panel, the number of thermoelectric modules should be 16/m². Lim et al. [5] developed an empirical model to predict energy consumption as well as the heating capacity of radiant panels in the heating mode. This prediction model can be integrated into building energy simulation programmes. Allouhi et al. [6] also found that the thermoelectric heating system can provide an energy savings of 55-64% compared to conventional electric heaters. Zuazua-Ros et al. [7] constructed a ventilated active thermoelectric envelope to assess its performance. Six TEMs were integrated into a building façade. Depending on the voltage input, they achieved a maximum COP of 2.1.

Liu et al. [8] worked on an open type of thermoelectric heating system with multiple channels. The effects of insulating layer thickness, airflow rates through the hot and cold sides, temperatures on the hot and cold sides, electric current direction, and numbers of TEMs were examined in the thermoelectric heating systems. This system attained an average heating coefficient of 1.3, which was higher than that of electric heating. Koochi et al. [9] designed a setup for space heating that consists of a thermoelectric system powered by a photovoltaic panel. Experimental investigation shows that a temperature difference of 6°C from the ambient temperature was observed with a maximum COP of 1.6 during the experiment period of 4 hours. Ibanez-Puy et al. [10] assert that it would be better to run the unit using more modules operating at lower voltage rather than fewer modules at higher voltage input. Wang et al. [11] performed tests in a room of 1 m³ and observed that for ambient temperatures ranging from 1 to 10°C, TE modules require high voltage (6–8 V) to ensure an adequate temperature level, whereas for ambient temperature greater than 10°C, more modules operating at low voltage (3–5 V) are required to make the system energy efficient.

Kim et al. [12] developed a model for a hydraulic thermoelectric radiant cooling system and found that cooling water temperature has the most significant influence on the COP of the system affecting it by 38.6–45.7%. Xie et al. [13] proposed a water-cooled thermoelectric component model which showed the increase in the COP and cooling capacity of TEC with increase in water flow rate and air flow rate. The earlier investigations, however, were carried out in low supply air conditions with low radiant surface temperatures. Few studies have been found using a water based heat sink for a thermoelectric radiant heating system inside a chamber. Water has higher heat carrying capacity than air, thus it is utilized in this study as the heat sink source. As a result, it is important to investigate the TERP's properties and assess how well it works in heating mode.

The study is focused on the thermal performance analysis of a thermoelectric radiant heating panel (TERHP) system in a test chamber for cold climatic conditions. The water block is used as a heat sink to maintain the temperature difference between the cold and hot sides of TEMs. The experiment is conducted by supplying inlet water at 18°C and applying operating voltages to the TERHP system of 12 V, 16 V, and 20 V. The surface temperature of panels, mean radiant temperature, operative temperature, air temperature, heating capacity, and coefficient of performance are measured on these inputs.

2. Methodology

The experiment is performed inside the insulated chamber of 1.2 x 1.2 x 2 m dimensions in the lab. There are three TE panels installed on the left, right, and front walls of the chamber.

2.1 Experimental setup description

The experimental setup includes TE radiant panels, a DC power supply, a water tank, submersible pumps, a water heater, a data logger, and a temperature controller as shown in Fig. 1. The radiant panel was constructed by attaching eight thermoelectric modules in a triangular arrangement to an aluminium panel of dimensions 0.75 x 0.50 m. According to a previous study, painting an aluminium panel black increased its heating performance by 2.3 to 2.8 times and its cooling performance by 1.5 to 1.7 times when compared to a non-painted panel [14]. Three TE radiant panels were painted matte black. The "I" water circulation circuit showed better performance in cooling studies. Water was supplied at 18°C, circulated in a closed loop. The experiment was conducted by applying operating voltages to the TERHP system of 12 V, 16 V, and 20 V in lab ambient temperatures of 17–18°C.

The study utilized a TEC1-12706 single-stage thermoelectric module with 127 semiconductor couples and 6 A current carrying capacity. The other technical parameters and their values are shown in Table 1. Thermal paste was applied on both sides of TEMs to attach the water block and metal panel surface to avoid internal resistance between them.

Q_{max} (W)	ΔT_{max} (K)	I_{max} (A)	V_{max} (V)	Resistance (Ω)	Size
50	66	6	14.4	1.98	4mm x 4mm x 3.9mm

Three TE radiant panels were electrically connected in parallel, having each TE panel with 8 TEMs in 4S x 2P configuration, as shown in Fig. 2 (b). Selected three pumps each having flow rate of 0.044 kg/s circulated water at a 0.0146 kg/s flow rate through each water block via smaller pipes connected with TE panels, as shown in Fig. 2 (a). which comes in range of 0.01 to 0.03 kg/s water flow rate as per previous studies through water blocks [16]. The remaining area of the rear side of the TE panels was thermally insulated.

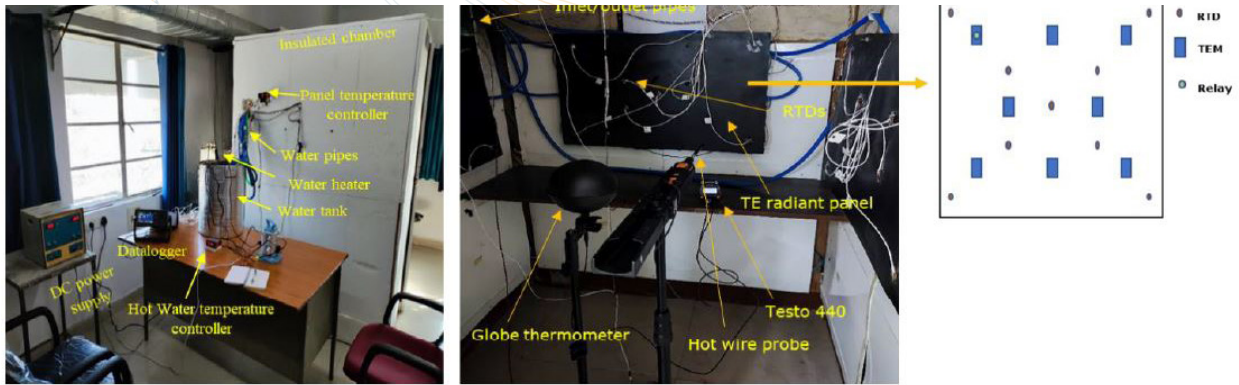


Figure 1: Outside and inside view of experimental setup for the present study and schematic of RTD placement on the TE panel

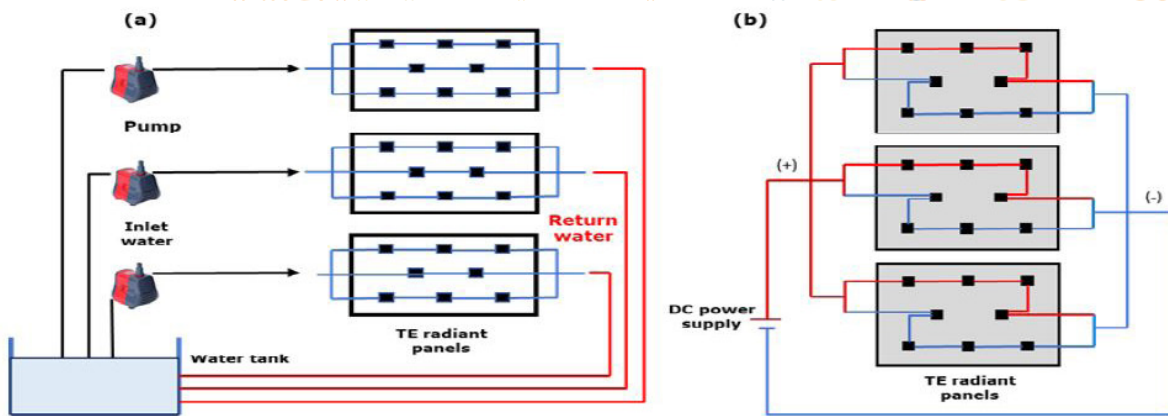


Figure 2: (a) Water circuit with "I" configuration and (b) Electric circuit for of TERHP system

Each thermoelectric radiant panel has nine RTD placed at positions as shown in Fig. 1 for better temperature measurement. Thus, the total number of RTDs attached to three radiant panels is 27. The spatial average is the number average of the air temperatures at the ankle level, the waist level, and the head level. These levels are 0.1, 0.6, and 1.1 m for seated occupants and 0.1, 1.1, and 1.7 m for standing occupants, according to ASHRAE. Four RTDs were attached vertically at these heights. One relay probe is attached to the center of the TEM as shown in Fig. 1 to maintain the required temperature on the TE radiant panel. One thermocouple was placed outside the test chamber to obtain ambient temperature data. A total of nine runs of experiments were performed for 12 V, 16 V, and 20 V. Each set of experiments is repeated three times with a water temperature range of 17-18°C for 2 hours each for a set point T_h value of 28°C, 30°C, and 33°C. Experiments utilized a DC power supply (Testronix 92 D), changing polarity for heating study, and recording temperature data using a data logger All temperature data were recorded by a data logger (Keysight DAQ973A, 20-channel multiplexer DAQM901A, 2 units) and Testo 440, a hotwire probe, and a globe thermometer for thermal comfort assessment.

2.2 Assumptions, duration, and measurements

The following assumptions were adopted during this experimental study:

- a) Thomson effect and heat losses by radiation and convection from the rear are neglected,

electric resistance and thermal conductivity of TEMs are constant.

- b) The Seebeck coefficients (α) of p- and n-type elements in TEMs are constant and equivalent.
- c) The temperatures of the bottom surface of the water block and panel surface are considered equal to the temperatures of the hot side and cold side of TEM, respectively.

In this study, the heating capacity and COP of a TE radiant panel were calculated. Temperature data were recorded mainly from the surface of the radiant panels. The heating capacity and COP of TEM ($Q_{h,panel}$, $COP_{h,panel}$) and TE radiant panels ($Q_{h,TEM}$, $COP_{h,TEM}$) can be calculated based on Equations (1)-(9) [12], [17-18]. Equations (5)-(10) were used in this study to calculate the heating capacity of the panel and COP. Terms used in the following equations were added in the nomenclature section.

$$Q_{h,TEM} = \alpha I T_h + 0.5 I^2 R - K(T_h - T_c) \tag{1}$$

$$Q_{c,TEM} = (T_{ws} - T_c)/R_w = \alpha I T_c - 0.5 I^2 R - K(T_h - T_c) \tag{2}$$

$$P_{TEM} = \alpha I (T_h - T_c) + I^2 R \tag{3}$$

$$COP_{h,TEM} = \frac{Q_{h,TEM}}{P_{TEM}} \tag{4}$$

$$Q_{h,rad} = \sigma A \epsilon (T_s^4 - MRT^4) \tag{5}$$

$$Q_{h,conv} = hA(T_s - T_{i,a}) \tag{6}$$

$$Q_{h,panel} = Q_{h,rad} + Q_{h,conv} \tag{7}$$

$$P_{panel} = V X I \tag{8}$$

$$COP_{h,panel} = \frac{Q_{h,panel}}{P_{panel}} \tag{9}$$

$$MRT = \left[(T_g + 273.15)^4 + \frac{(0.25 \times 10^8)}{\epsilon_g} \left(\frac{|T_g - T_{i,a}|}{D} \right)^{\frac{1}{4}} (T_g - T_{i,a}) \right]^{\frac{1}{4}} - 273.15 \tag{10}$$

$$T_{op} = \frac{T_a + MRT}{2} \tag{11}$$

$$Nu = 0.59 (Ra)^{0.25} \text{ for } 10^4 < Ra < 10^9 \tag{12}$$

Heating experiments were performed in the lab-based test chamber during February of the winter season. The data was logged at a 10 second interval during the experiment. The current values were noted, corresponding to the applied voltage in the DC power supply. As the three TE radiant panels were electrically connected in parallel, the operational voltages for the experiment were selected as 12 V, 16 V, and 20 V, considering panel surface temperature and COP variations. The minimum and maximum operational voltages for the study are selected as 12 V and 20 V, respectively. Maximum panel temperature was achieved as 27.45°C and 32.30°C at 12 V and 20 V, respectively, which comes under the same range selected in previous research for heating mode [19]. Thus, a 2-hour experiment was performed to achieve these surface temperatures. Rayleigh number at all voltages found to be in the range of 104 to 108 thus for vertical mounted panels Nusselt number was calculated using Equation (12).

A combination of random error (py) and propagation error (by) results in the total uncertainty (Uy) of measured values, as shown in equation (13). According to Equation (2), the propagation error (by) is calculated by a constant error term (bxi) that is obtained by multiplying the temperature sensor error by the standard deviation of the measured temperature (Sr). Equation (14), which includes the standard deviation and mean value (M) of the measurements, defines the random error (Py) [20]. Total uncertainty is shown for measured parameters in Table 2.

$$U_y = \sqrt{(b_y^2 + p_y^2)} \tag{13}$$

$$b_y = \sqrt{\left[\sum_{i=1}^n \left(\frac{dy}{dx_i} b_{x_i} \right)^2 \right]}, p_y = \frac{2S_r}{\sqrt{M}} \tag{14}$$

Parameters	Uncertainty
Temperatures	0.2-0.5°C
Heating capacity (Q_h)	0.067 W
COP_h	0.06

3. Results

Testing of the radiant panels is performed under three voltage inputs of 12, 16, and 20 V, with an initial indoor temperature kept at $20.6 \text{ }^\circ\text{C} \pm 0.1^\circ\text{C}$. MRT , $Q_{h,panel}$ and $COP_{h,panel}$ were computed using Equations (10), (7), and (9) in accordance with T_s , $T_{i,a}$, T_g and the current measured during the test. The variation of panel temperature under different voltages of the experiment during the period of 2 hours is shown in Fig. 3(a). For the first 830 seconds, the panel temperature rises sharply, and as time passes, the rise of the panel surface continues but at a slower rate.

The variation of the mean radiant temperature under the applied input voltage is shown in Fig. 3(b). The mean radiant temperature (MRT) increases with the increase in panel surface temperature with respect to time, as there is no other heating source except the panel. Indoor air temperature increments under different input voltages are shown in Fig. 3(c). The maximum indoor temperature increment for 12 V, 16 V, and 20 V was $2.06 \text{ }^\circ\text{C}$, $2.86 \text{ }^\circ\text{C}$, and $4.02 \text{ }^\circ\text{C}$, respectively. Operative temperature was calculated using Equation (11) which is the mean of the indoor air temperature and the MRT. Operative temperature shows a similar kind of variation as obtained in MRT, as shown in Fig. 3(d).

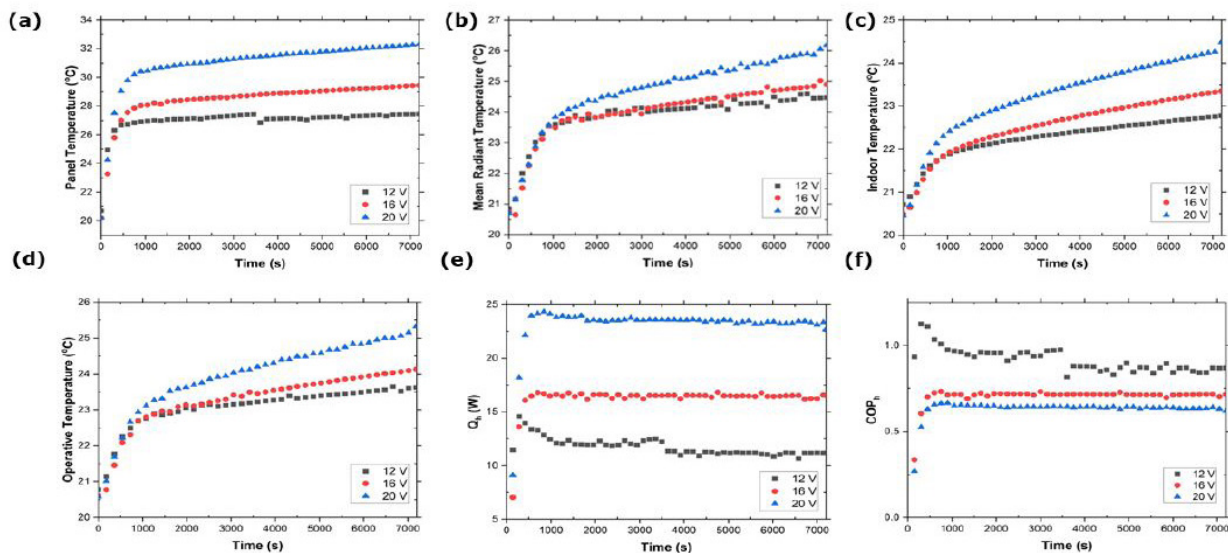


Figure 3: Temporal variation of (a) Panel Temperature (b) Mean Radiant Temperature (c) Indoor Temperature (d) Operative Temperature (e) Heating Capacity (Q_h) of TE panel (f) COP_h of TE panel

Increasing the voltage value raises the current, which increases the temperature differential due to the Peltier effect, resulting in a higher temperature on the hot side of the module. The change in the heating capacity under different voltages with respect to time is shown in Fig. 3(e). Heating capacity for the higher input voltage can be seen to be higher, and it first increases very sharply with time, reaches a maximum value, and then starts to decrease at a slower rate as the difference between indoor air temperature and panel temperature decreases. The maximum heating capacity obtained was 14.7 W, 17.13 W, and 24.41 W for 12, 16, and 20 V, respectively.

COP_h , depending on the heating capacity, shows similar variation for constant input electrical voltage (V) with respect to time, it first increases and reaches a maximum value, after that, the COP_h decreases. The maximum COP_h was found to be 1.14, 0.74, and 0.66 for 12, 16, and 20 V respectively. COP_h decreases with an increase in the input electrical voltage, as can be observed from Fig. 3(f). This shows that the increase in the heating capacity is less as compared to the voltage applied or power input.

The temperature distribution at the active side of the panel at different voltage values of 12 V, 16 V, and 20 V captured by a thermal camera is shown in Fig. 5, which is nearly the same as measured by RTDs. The vertical air temperature at heights of 0.1 m, 0.6 m, 1.1 m, and 1.7 m is shown in Fig. 5 with respect to 12 V, 16 V, and 20 V. The vertical air temperature distribution was obtained for the sitting and standing positions of a person according to ASHRAE.

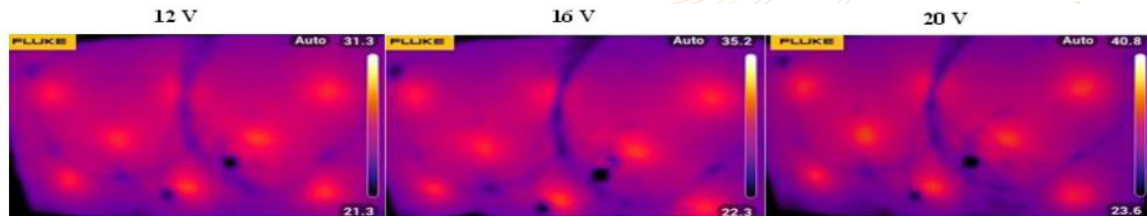


Figure 4: IR camera images of actual temperature distribution at the active side of panel at 12 V, 16 V and 20 V.

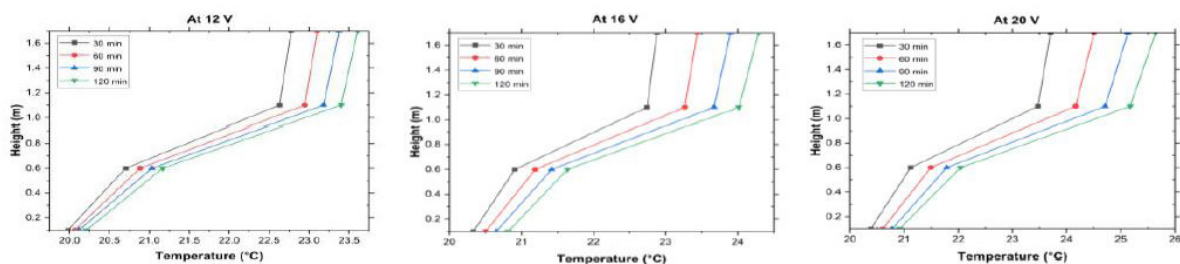


Figure 5: Vertical air temperature distribution at 12 V, 16 V and 20 V

4. Discussion

The indoor temperature rise occurred due to heat exchange between the TE panels and the study chamber. As the temperature difference between the hot and cold sides of TEM increases, TE modules require more energy to push electrons from the cold side to the hot side. A high supply voltage is required for higher surface temperatures. As shown in Fig. 3(a), the panel temperature rises sharply for 830 seconds because, ΔT_{TEM} increases fast, and then the rise of the panel surface continues but at a slower rate because of stable ΔT_{TEM} . The cold-side temperature is maintained with a supply of constant temperature water. MRT, indoor air temperature, and operative temperature increase with time, as shown in Figs. 3 (b) - 3 (d).

According to ASHRAE, the inside design condition for winter with a 90% acceptability requirement is that the operative temperature persists within a range of 20–23.5°C for a 0.9 clo condition with an occupancy having activity less than 1.2 met. The upper limit of 23.5°C is achieved within 98 minutes, 59 minutes, and 27 minutes at 12 V, 16 V, and 20 V, respectively. The desired value of operative temperature is achieved in less than 2 hours at the lowest voltage, i.e., 12 V, with the present setup. The preceding line illustrates that to obtain the necessary operative temperature within the range of thermal comfort at a faster pace, power input must be increased, which comes at the expense of a low COP value. Optimization of the TE radiant heating panel necessitates a trade-off between COP and power input to TEM, which is dependent on ambient temperature, duration, and power cost.

Heating capacity, which is the combined effect of radiation and convection near the TE panel, initially rises fast, then goes down and becomes nearly constant because panel surface temperature rises at a faster rate initially than MRT and air temperature; further, all three temperatures rise slowly. With higher voltage selection, power consumption for the panel increases, leading to a decrease in COP at higher voltages, as shown in Fig. 3(f). The power supplied to each TE panel is 12.84 W, 23.09 W, and 36.66 W. Air with a high temperature is lighter, and due to the density difference, buoyant forces act upon it, raising it to a higher level.

5. Conclusion

This paper experimentally examines the thermal performance of a thermoelectric radiant panel system for indoor space heating. The heating performance of the TERHP system in a test chamber with designed TE radiant panels for optimum voltage or energy-efficient criteria was investigated. The outcomes of this study are concluded as follows:

- At 12 V, the TERHP system attained the highest COP of 1.14, which suggests that at lower voltages, the energy efficiency of the system increases, while for higher heating requirements at lesser energy efficiency, 20 V or high voltages should be supplied to the TERHP system. Thus, the electric connection of TEMs in a TE panel is important for determining the energy efficiency of the system.
- A water-based heat sink enhances TERHP system COP and heating capacity more than an air-based one used in previous studies. Water supply temperature (T_{ws}) should be near to ambient temperature for a higher COP of the system, and for higher heating capacity, a high T_{ws} can be selected. In this study, water at 17-18°C was supplied. With a high figure of merit, better COP and heating capacity are expected with TEM.
- In this study, the upper limit of thermal comfort temperature (i.e., T_{op}) at the highest voltage was achieved within 27 minutes. The same level of thermal comfort can be achieved by a TERHP system at a lower air temperature. This results in lower energy consumption.

6. Nomenclatures

α	Seebeck coefficient (V/K)	R	Electric resistance of TEM (Ω)
K	Thermal conductivity ($W/m^2 \cdot K$)	R_w	Thermal resistance of water block (K/W)
V	DC voltage supplied to each TE panel (V)	I	Input current to each TE panel (A)
T_h	Hot side temperature of TEM (K)	T_c	Cold side temperature of TEM (K)
T_s	TE panel surface temperature (K)	$T_{i,a}$	Indoor air temperature (K)
T_g	Globe temperature (K)	T_{ws}	Supply water temperature (K)
MRT	Mean radiant temperature (K)	T_{op}	Operative temperature (K)
ϵ_g	Emissivity of globe thermometer	D	Globe diameter (m)
Nu	Nusselt number	Ra	Rayleigh number
A	TE panel area (m^2)		

7. Acknowledgement

The authors would like to express their sincere gratitude to the Department of Science and Technology, Government of India, for the research grant DST/TMD/CERI/RES/2020/40(G) for the financial support of the thermoelectric radiant heating system studies at the Centre for Energy and Environment, MNIT Jaipur.

8. References

- [1] The Kigali Amendment (2016): The amendment to the Montreal Protocol agreed by the Twenty-Eighth Meeting of the Parties (Kigali, 10-15 October 2016) | Ozone Secretariat. Retrieved November 9, 2023, from <https://ozone.unep.org/treaties/montreal-protocol/amendments/kigali-amendment-2016amendment-montreal-protocol-agreed>
- [2] Dhamodharan, P., Ayalur, B. K., Judefelix, J., Prabakaran, R., & Kim, S. C. (2024). Energy saving potential in radiant cooling system by utilizing air-conditioning condensate: A strategy for green building rating. *Applied Thermal Engineering*, 236, 121492. <https://doi.org/10.1016/j.applthermaleng.2023.121492>
- [3] Cosnier, M., Fraisse, G., & Luo, L. (2008). An experimental and numerical study of a thermoelectric aircooling and air-heating system. *International Journal of Refrigeration*, 31(6), 1051-1062. <https://doi.org/10.1016/J.IJREFRIG.2007.12.009>

- [4] Shen, L., Tu, Z., Hu, Q., Tao, C., & Chen, H. (2017). The optimization design and parametric study of thermoelectric radiant cooling and heating panel. *Applied Thermal Engineering*, 112, 688–697. <https://doi.org/10.1016/J.APPLTHERMALENG.2016.10.094>
- [5] Lim, H., & Jeong, J. W. (2020). Numerical and Experimental Study on the Performance of Thermoelectric Radiant Panel for Space Heating. *Materials* 2020, Vol. 13, Page 550, 13(3), 550. <https://doi.org/10.3390/MA13030550>
- [6] Allouhi, A., Boharb, A., Ratlamwala, T., Kousksou, T., Amine, M. B., Jamil, A., & Msaad, A. A. (2017). Dynamic analysis of a thermoelectric heating system for space heating in a continuous-occupancy office room. *Applied Thermal Engineering*, 113, 150–159. <https://doi.org/10.1016/J.APPLTHERMALENG.2016.11.001>
- [7] Zuazua-Ros, A., Martín-Gómez, C., Ibáñez-Puy, E., Vidaurre-Arbizu, M., & Ibáñez-Puy, M. (2018). Design, assembly and energy performance of a ventilated active thermoelectric envelope module for heating. *Energy and Buildings*, 176, 371–379. <https://doi.org/10.1016/J.ENBUILD.2018.07.062>
- [8] Liu, D., Zhao, F. Y., Yang, H., & Tang, G. F. (2015). Theoretical and experimental investigations of thermoelectric heating system with multiple ventilation channels. *Applied Energy*, 159, 458–468. <https://doi.org/10.1016/J.APENERGY.2015.08.125>
- [9] Koohi, N., Nasirifar, S., Behzad, M., & Cardemil, J. M. (2021). Experimental investigation and performance assessment of a solar-driven thermoelectric unit for localized heating and cooling applications. *Energy and Buildings*, 253, 111517. <https://doi.org/10.1016/J.ENBUILD.2021.111517>
- [10] Ibañez-Puy, M., Bermejo-Busto, J., Martín-Gómez, C., Vidaurre-Arbizu, M., & Sacristán-Fernández, J. A. (2017). Thermoelectric cooling heating unit performance under real conditions. *Applied Energy*, 200, 303–314. <https://doi.org/10.1016/J.APENERGY.2017.05.020>
- [11] Wang, C., Calderón, C., & Wang, Y. D. (2017). An experimental study of a thermoelectric heat exchange module for domestic space heating. *Energy and Buildings*, 145, 1–21. <https://doi.org/10.1016/J.ENBUILD.2017.03.050>
- [12] Kim, M., Kang, Y. K., Joung, J., & Jeong, J. W. (2022). Cooling Performance Prediction for Hydraulic Thermoelectric Radiant Cooling Panels with Experimental Validation. *Sustainability* 2022, Vol. 14, Page 16214, 14(23), 16214. <https://doi.org/10.3390/SU142316214>
- [13] Xie, X., Zhang, X., Zhang, J., Qiao, Q., Jia, Z., Wu, Y., ... & Li, Q. (2023). Performance analysis and optimal design of a water-cooled thermoelectric component for air cooling based on simulation and experiments. *International Communications in Heat and Mass Transfer*, 141, 106576. <https://doi.org/10.1016/j.icheatmasstransfer.2022.106576>
- [14] Amanowicz, Ł., & Wojtkowiak, J. (2018). Experimental investigations of thermal performance improvement of aluminum ceiling panel for heating and cooling by covering its surface with paint. *E3SWC*, 44, 00002. <https://doi.org/10.1051/E3SCONF/20184400002>
- [15] TEC1-12706 Datasheet (PDF) - HB Electronic Components. (n.d.). Retrieved July 24, 2023, from <https://www.alldatasheet.com/datasheet-pdf/pdf/313841/HB/TEC1-12706.html>
- [16] Lim, H., Cheon, S. Y., & Jeong, J. W. (2018). Empirical Analysis for the Heat Exchange Effectiveness of a Thermoelectric Liquid Cooling and Heating Unit. *Energies* 2018, Vol. 11, Page 580, 11(3), 580. <https://doi.org/10.3390/EN11030580>
- [17] Aparicio, P., Salmerón, J. M., Ruiz, Á., Sánchez, F. J., & Brotas, L. (2016). The globe thermometer in comfort and environmental studies in buildings. *Revista de La Construcción*, 15(3), 57–66. <https://doi.org/10.4067/S0718-915X2016000300006>

- [18] C.P. Kothandaraman & S. Subramanyan. (2007). Heat and Mass Transfer Data Book 6th Edition. New Age International (P) Ltd., Publishers, 1-14. https://books.google.com/books/about/Heat_and_Mass_Transfer_Data_Book.html?id=5FKaEznxsSMC
- [19] Shen, L., Xiao, F., Chen, H., & Wang, S. (2013). Investigation of a novel thermoelectric radiant airconditioning system. *Energy and Buildings*, 59, 123-132. <https://doi.org/10.1016/J.ENBUILD.2012.12.041>
- [20] Lim, H., Lee, S. J., Su, Y., & Jeong, J. W. (2022). Experimental study and prediction model of a liquid desiccant unit for humidification during the heating season. *Journal of Building Engineering*, 45, 103549. <https://doi.org/10.1016/J.JOBE.2021.103549>